Study of the H−F Stretching Band in the Absorption Spectrum of $(CH_3)_2O\cdots HF$ in the Gas Phase

V. P. Bulychev, E. I. Gromova, and K. G. Tokhadze*

Institute of Physics, St. Petersburg State University, Peterhof, St. Petersburg, 198504 Russia

Received: August 30, 2007; In Final Form: October 31, 2007

The absorption spectra of the $(CH_3)_2O\cdots HF$ complex in the range of 4200−2800 cm^{-1} were recorded in the gas phase at a resolutions of 0.1 cm^{-1} at $T = 190-340$ K. The spectra obtained were used to analyze their structure and to determine the temperature dependencies of the first and second spectral moments. The band shape of the $(CH_3)_2O\cdots HF$ complex in the region of the ν_1(HF) stretching mode was reconstructed nonempirically. The ν_1 and ν_3 stretching vibrations and four bending vibrations responsible for the formation of the band shape were considered. The equilibrium geometry and the 1D−4D potential energy surfaces were calculated at the MP2 6-311++G(2d,2p) level with the basis set superposition error taken into account. On the basis of these surfaces, a number of one- and multidimensional anharmonic vibrational problems were solved by the variational method. Solutions of auxiliary 1D and 2D vibrational problems showed the strong coupling between the modes. The energy levels, transition frequencies and intensities, and the rotational constants for the combining vibrational states necessary to reconstruct the spectrum were obtained from solutions of the 4D problem (ν_1, ν_3, $\nu_5(B_2)$, $\nu_6(B_2)$) and the 2D problem ($\nu_5(B_1)$, $\nu_6(B_1)$). The theoretical spectra reconstructed for different temperatures as a superposition of rovibrational bands associated with the fundamental, hot, sum, and difference transitions reproduce the shape and separate spectral features of the experimental spectra. The calculated value of the ν_1 frequency is 3424 cm^{-1}. Along with the frequencies and absolute intensities, the calculation yields the vibrationally averaged values of the separation between the centers of mass of the monomers *R*c.-of-m., *R*(O···F), and *r*(HF) for different states. In particular, upon excitation of the ν_1 mode, *R*c.-of-m. becomes shorter by 0.0861 Å, and *r*(HF) becomes longer by 0.0474 Å.

Introduction

Spectroscopic studies of the $(CH_3)_2O\cdots HF$ complex of dimethylether with hydrogen fluoride with a moderately strong hydrogen bond were started about 40 years ago. Together with the related complexes $H_2O\cdots HF$ and $HCN\cdots HF$, this complex belongs to a few H-bonded systems whose infrared absorption spectra can be recorded in the gas phase. Nonetheless, the studies of spectra of the $(CH_3)_2O\cdots HF$ complex available at present in the literature are not numerous. To date, certain information is obtained on the fundamental band and the first overtone band of the ν_{HF} (ν_{DF}) stretching vibration,[1−3] the δ_{HF} bending vibration,[4] and the low-frequency ν_σ stretching vibration of the hydrogen bond.[5] The gas-phase studies were supplemented with measurements of spectra of the $(CH_3)_2O\cdots HF$ complex in low-temperature matrices[6] at $T = 12$ K and in solution in liquefied xenon[7,8] at $T = 210-260$ K. Analysis of the available experimental data shows that the anharmonic interaction of the high-frequency $\nu_{HF} \equiv \nu_1$ and low-frequency modes is a governing factor in the formation of spectra of such complexes.

It should be noted that the absorption bands associated with the combination (sum and difference) $\nu_1 \pm \nu_3$ transitions can be recorded reliably by studying the $(CH_3)_2O\cdots HF$ complex. Here, ν_3 is the intermolecular stretching vibration. These bands were, for the first time, observed[1] in the range of 3900−3100 cm^{-1} against a background of the wide asymmetric ν_1 stretching band. The distinct maximum on the high-frequency wing of the spectrum is assigned to the $\nu_1 + \nu_3$ sum band, while the weak absorption on the low-frequency wing is associated with the $\nu_1 - \nu_3$ difference band. The frequency of the ν_3 mode in the complex of HF with $(CH_3)_2O$ was estimated[1] to be about 170 cm^{-1}. The spectra of mixtures of HF(DF) with dimethylether in the far-infrared region of 50−350 cm^{-1} were recorded,[5] and for the $(CH_3)_2O\cdots HF(DF)$ complexes, the ν_3 frequency was found to be 185 ± 10 cm^{-1}, which is close to the estimate.[1] On the basis of the temperature dependences of the absorption bands of free molecules and complexes,[5] the energy of formation of the complexes in the gas phase of $D = 43$ kJ $mol^{-1} = 10.28$ kcal $mol^{-1} = 3590$ cm^{-1} was derived. Finally, the frequencies of absorption bands associated with the high-frequency ν_5 bending vibration of hydrogen fluoride were found to be 755 and 665 cm^{-1} in $(CH_3)_2O\cdots HF$ and 550 and 490 cm^{-1} in $(CH_3)_2O\cdots DF$.[4]

The ν_1 band shape of the $(CH_3)_2O\cdots HF$ complex does not change on the whole upon transition from the gas phase to solution in liquefied Xe,[7,8] which is one of the simplest solvents. A high-frequency maximum at 3610 cm^{-1} associated with the $\nu_1 + \nu_3$ transition is observed against the background of the central component of cryospectra at about 3380 cm^{-1}. The $\nu_1 + \nu_3$ band is not observed in the Ar matrix[6] at $T = 12$ K. Under these conditions, a narrow ν_1 band of the complex is recorded at 3350 cm^{-1}, which reveals a certain asymmetry.

In recent decades, considerable attention has been given to analysis of the mechanisms forming the complicated ν_1 absorption band of the complex and to attempts to describe it in terms of anharmonic models. The temperature dependence of the ν_{HF} band shape in the $(CD_3)_2O\cdots HF$ complex was studied[7,8] in the

* To whom correspondence should be addressed.

10.1021/jp076966f CCC: $40.75
Published on Web 01/23/2008

gas phase in the temperature range of 220−360 K. Upon passage to low temperatures, additional spectral features of the band appeared, which facilitated the interpretation of the band structure. The profile of the absorption band in the region of the stretching frequency of hydrogen fluoride in the complex was reconstructed[7] with the use of a semiempirical model, taking into account the coupling of the ν_1 vibration to the ν_3 vibration and to the low-frequency $\nu_6(B_1)$ and $\nu_6(B_2)$ bending vibrations of dimethylether, as distinct from earlier studies[1−3] where only the interaction with the ν_3 vibration was considered. Along with the fundamental $v_1 = 0 \rightarrow 1$ transition, a set of hot transitions with the frequencies

$$\nu_1 + x_{13}\cdot v_3 + x_{16(B_1)}\cdot v_6(B_1) + x_{16(B_2)}\cdot v_6(B_2) \qquad (1)$$

was taken into account, as well as the sum and difference transitions with the frequencies

$$\nu_1 + \nu_k + x_{1k} + x_{13}\cdot v_3 + x_{16(B_1)}\cdot v_6(B_1) + x_{16(B_2)}\cdot v_6(B_2) \qquad (2)$$

and

$$\nu_1 - \nu_k + x_{13}\cdot v_3 + x_{16(B_1)}\cdot v_6(B_1) + x_{16(B_2)}\cdot v_6(B_2) \qquad (3)$$

The rotational structure of vibrational bands was also considered. In eqs 1−3, v_k is the vibrational quantum number, and x_{1k} is the anharmonicity constant. The intensities of individual transitions $|0\ v_3\ v_{6(B_1)}\ v_{6(B_2)}\rangle \rightarrow |1\ v'_3\ v'_{6(B_1)}\ v'_{6(B_2)}\rangle$ are determined by the population of initial energy levels, the squares of the transition dipole moments, and the electro-optical anharmonicity constants.[9]

The profile of the ν_{HF} band and its temperature variations were satisfactorily described[7] in terms of this model with the use of the spectral parameters $\nu_1 = 3430 \pm 5$, $\nu_3 = 165 \pm 5$, $\nu_6(B_1) = 60 \pm 5$, $\nu_6(B_2) = 30$, $x_{13} = 70 \pm 5$, $x_{16(B_1)} = 2.5$, and $x_{16(B_2)} = 1.8$ cm^{-1}. Some of the parameters were derived directly from the experiment, and the other parameters were found from fitting the calculated spectra to the experimental spectra. When calculating the band shapes, the following changes in the rotational constant B upon transitions between vibrational states were taken into account: 0.007 (the $v_1 = 0 \rightarrow 1$ transition), 0.005 (the $v_1 = 0$, $v_3 = 0 \rightarrow v_1 = 1$, $v_3 = 1$ transition), and 0.009 cm^{-1} (the $v_1 = 0$, $v_3 = v_1 = 1$, $v_3 = 0$ transition). These increments were found while analyzing the rotation−vibration spectrum of the complex.

The absorption spectra of the $(CH_3)_2O\cdots HF$ complex in the range of 3700−3200 cm^{-1} were recorded[10] in a gas cell at $T =$ 188−271 K and in a supersonic jet (mixtures of $(CH_3)_2O$, HF, and Ar) at $T \leq 70$ K. The structural details associated with the contributions of different vibrational transitions are the most distinct in the spectra recorded in the supersonic jet, although under these conditions, the bands of separate transitions overlap to some degree. The experimental studies were supplemented with quantum chemical calculations of the equilibrium geometry of the monomers and the complex at the DFT and MP2 levels. On the basis of the calculated results and the temperature behavior of the spectra, the authors[10] carefully interpreted the structure of absorption bands and derived the frequencies of the most important sum, difference, combination, and hot transitions. As in the study,[7] the theoretical spectra were constructed as a superposition of the fundamental band with $\nu_1 = 3428.5$ cm^{-1} and the vibrational bands arising due to the coupling of the high-frequency stretch of HF to the ν_3 intermolecular stretch and to an intermolecular bending vibration denoted by ν_δ. Thus, the authors[10] somewhat simplified the problem and did not discriminate between the $\nu_6(B_1)$ and $\nu_6(B_2)$ vibrations occurring in the mutually perpendicular planes. When fitting the theoretical spectra to the experimental data, the intensities of separate bands were found by using the technique of variable overlap integrals of the wave functions of combining states of the low-frequency modes. The constant of anharmonic coupling of the ν_1 and ν_δ vibrations is found to be $x_{1\delta} = 10.5-13.0$ cm^{-1}, the estimate of x_{13} is 33 ± 2 cm^{-1}, and the difference between the frequencies of the $|000\rangle \rightarrow |110\rangle$ and $|000\rangle \rightarrow |100\rangle$ transitions is 199 cm^{-1}. The procedure employed allowed the authors to construct the theoretical spectra in good agreement with the experimental data for both the gas cell and supersonic jet experiments.

It is evident that the simplified schemes with fixed values of the frequencies of the intermolecular modes and the anharmonicity constants and with a parametric representation of transition intensities cannot describe, in detail, the complicated band shape of the $(CH_3)_2O\cdots HF$ complex. It was shown[11,12] that the complicated band shape of the $H_2O\cdots HF$ complex can be described with a good accuracy in the framework of a totally nonempirical calculation. In particular, the assignment of structural features of the $H_2O\cdots HF$ spectrum was refined in these papers. These results were confirmed by the independent calculation and the low-temperature experiment.[13] The purpose of the present paper is to obtain additional experimental information on the spectra of the $(CH_3)_2O\cdots HF$ complex in the gas phase, in particular, at higher temperatures, and to perform a nonempirical calculation of the electro-optical parameters of the complex necessary to reconstruct the absorption band in the region of the ν_1 fundamental transition.

Experimental Section

The spectra in the range of 4200−2800 cm^{-1} were recorded with Bruker IFS-113v and Bruker IFS-120 HR vacuum Fourier spectrometers at a resolution of about 0.1 cm^{-1}. A stainless steel cell ($L = 20$ cm) with CaF_2 windows was used to record the gas-phase spectra in the temperature interval of 190−340 K. The partial pressures were $p(HF) \sim 5-10$ Torr and $p((CH_3)_2O) \sim 40-60$ Torr. The pressures of the components were chosen in such a way[10,12,14] as to exclude the appearance of complicated complexes containing more than two HF molecules. The changes in the concentrations of components in the course of the experiment did not exceed one percent.

The experimental absorption spectra of mixtures $(CH_3)_2O$/HF recorded at $T = 190$, 230, 285, and 320 K are shown in Figures 1 and 2, together with the theoretical spectra of the $(CH_3)_2O\cdots HF$ complex calculated for these temperatures. The method used to calculate the spectra and their discussion will be presented below. The band in question of the $(CH_3)_2O\cdots HF$ complex lies in the region of 3900−3200 cm^{-1} and overlaps the P branch of the rovibrational absorption band of free HF molecules. The relatively weak rovibrational lines $P(3)-P(8)$ that fall on the high-frequency wing of the ν_1 band were subtracted by using the approach described earlier.[15]

One can see in Figures 1 and 2 that the absorption band of the ν_1 stretch in the $(CH_3)_2O\cdots HF$ complex has a complicated shape. It contains the intense, asymmetric central component with a maximum at 3450−3460 cm^{-1}, the high-frequency component in the region of 3700 cm^{-1}, and the weakly pronounced low-frequency component at 3300 cm^{-1}. For convenience, we indicate in the figures the frequency ν_1^0 of the vibrational transition from the ground vibrational state and the regions of formation of the sum (I and II) and difference (III and IV) bands[7,8,10] involving the stretching and bending

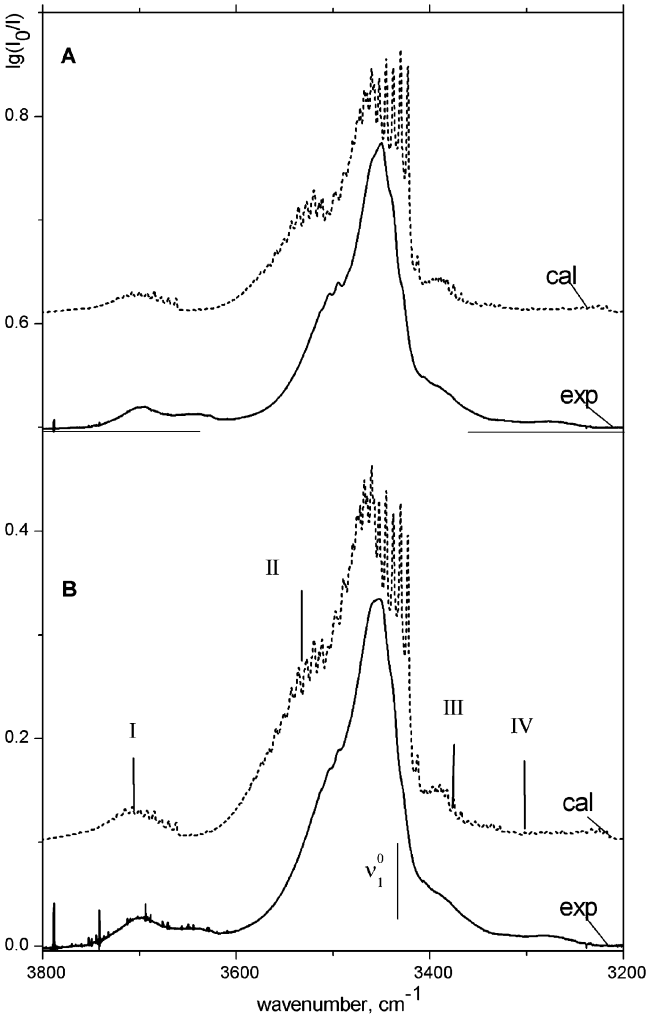

Figure 1. Experimental and theoretical absorption spectra of the $(CH_3)_2O\cdots HF$ complex in the gas phase in the region of the ν_1 mode at $T = 190$ (A) and 230 K (B).

intermolecular vibrations. The central component has a low-frequency shoulder and an extended high-frequency wing. The positions of the main maxima virtually do not depend on the concentration of components of a gaseous mixture and the temperature of a sample. As the temperature decreases, structural features appear on the high-frequency wing of the central component in the region of 3500 cm^{-1}. Unfortunately, it is practically impossible to decrease the temperature below 190 K under stationary conditions since the saturation vapor pressure of $(CH_3)_2O\cdots HF$ complexes becomes very low and the weak band of the complex cannot be recorded even by the Fourier spectroscopy technique.

Information useful for comparison of theoretical and experimental results can be obtained from analysis of the first and second spectral moments and their temperature dependences.[16,17] From the experimental spectra, we evaluated the first moment that determines the center of gravity υ_0 of the band

$$M_1^* = M_0^{-1} \int_{\upsilon_1}^{\upsilon_2} \upsilon \cdot D(\upsilon) \mathrm{d}\upsilon = \upsilon_0 \qquad (4)$$

where $D(\upsilon) = \lg(I_0/I)$ and

$$M_0 = \int_{\upsilon_1}^{\upsilon_2} D(\upsilon) \mathrm{d}\upsilon$$

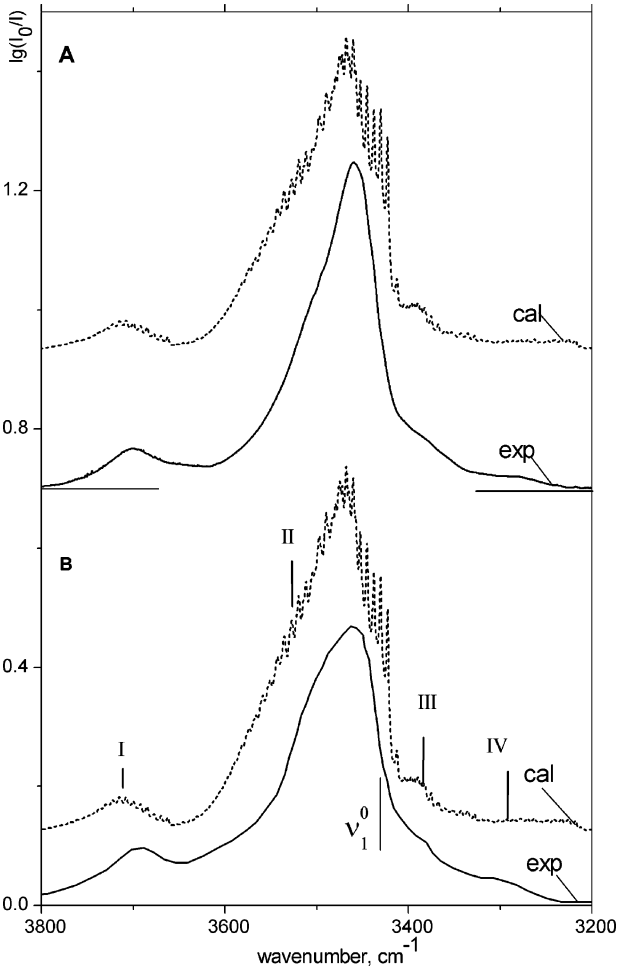

Figure 2. Experimental and theoretical absorption spectra of the $(CH_3)_2O\cdots HF$ complex in the gas phase in the region of the ν_1 mode at $T = 285$ (A) and 320 K (B).

TABLE 1: Experimental and Theoretical Values of Spectral Moments M_1^* and M_2^* and the Effective Width $\Delta\upsilon_{1/2}$ of the ν_1 Band of the $(CH_3)_2O\cdots HF$ Complex at Different Temperatures[a]

T (K)	M_1^* (cm^{-1})		M_2^* (cm^{-2})		$\Delta\upsilon_{1/2}$ (cm^{-1})	
	exp	theor	exp	theor	exp	theor
190	3470	3478	4400	6685	130	164
230	3480	3481	5900	7200	155	170
285	3490	3485	8700	7694	180	175
320	3510	3487	12500	7949	220	178

[a] Note: Experimental errors of M_1^*, M_2^*, and $\Delta\upsilon_{1/2}$ increase with temperature and lie in the intervals of 2−3 cm^{-1}, 15−20%, and 10−20 cm^{-1}, respectively.

is the integral intensity of the band, and the second spectral moment

$$M_2^* = M_0^{-1} \int_{\upsilon_1}^{\upsilon_2} (\upsilon - \upsilon_0)^2 \cdot D(\upsilon) \mathrm{d}\upsilon \qquad (5)$$

that characterizes the effective width of the band $\Delta\upsilon_{1/2} = 2\sqrt{M_2^*}$. Integration was performed over the frequency range of 3100−3900 cm^{-1}. The values of normalized moments for different temperatures are presented in Table 1. The error of evaluation of υ_0 does not exceed 3 cm^{-1}, and the inaccuracy of the determination of M_2^* amounts to 15−20%. One can see from Table 1 that the center of gravity of the band significantly shifts to higher frequencies and that the band broadens with increasing temperature.

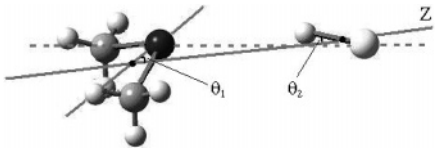

Figure 3. Equilibrium geometry of the $(CH_3)_2O\cdots HF$ complex. The solid line Z goes through the centers of mass of $(CH_3)_2O$ and HF; the dashed line joins the O and F atoms.

Nonempirical Calculation of the Electro-optical Parameters of the $(CH_3)_2O\cdots HF$ Complex. *(1) Ab Initio Calculation of the Equilibrium Geometry of the Complex.* The electronic structure calculation of the complex was carried out using the Gaussian03 package of codes[18] at the MP2 6-311++G(2d,2p) level with the basis set superposition error (BSSE) taken into account by the counterpoise method.[19] It is known[10,20] that using the 6-311++G(2d,2p) set of atomic functions allows the properties of molecular complexes of this type to be calculated with good accuracy. Like the complex of water with hydrogen fluoride, the $(CH_3)_2O\cdots HF$ complex has two equivalent nuclear configurations corresponding to the minimum-energy value. Each configuration possesses the symmetry properties of the C_s group. One of the possible configurations is shown in Figure 3. The potential energy barrier between the two nuclear configurations equals 153 (without the BSSE correction) and 196 cm^{-1} (with this correction). These values were computed at the indicated level of theory, assuming that the atoms of the HF molecule lie on the line joining the centers of gravity of the monomers and that the other geometrical parameters have the equilibrium values.

The equilibrium values of interatomic distances and angles obtained in our calculation are in good agreement with the available literature data.[10,21] For example, $r(OC) = 1.425$ Å, $r(CH) = 1.083$, 1.089, 1.089 Å (for three CH bonds of a CH_3 group), $r(HF) = 0.939$ Å, the distance R between the centers of gravity of the monomers equals 3.003 Å, and the angle between the symmetry axis of $(CH_3)_2O$ and the O···F line is 143°. For this geometry, the energy of the complex is −254.98242722 au, and the dipole moment is 4.43 D. The isolated HF molecule calculated at this level of theory has the energy of −100.303060 au, the dipole moment of 1.982 D, and the bond length of 0.9178 Å. Thus, the HF molecule increases its bond length by 0.021 Å upon complexation with the $(CH_3)_2O$ molecule. For an isolated $(CH_3)_2O$ molecule, the equilibrium bond lengths are $r(OC) = 1.416$ Å, $r(CH) = 1.084$, 1.092, 1.092 Å, and the energy equals −154.6647544 au. The theoretical value of the stabilization energy of the complex is 0.0146 au = 9.17 kcal mol^{-1}, which is in agreement with the experimental[5] estimate of 10.28 kcal mol^{-1} and a theoretical[21] value of 9.41 kcal mol^{-1}. Thus, the method adopted here to calculate the geometry of the $(CH_3)_2O\cdots HF$ complex and its electronic energy (the potential energy of vibrations) is sufficiently accurate. The same method was used below to calculate sections of the potential energy surface (PES).

(2) Solution of Auxiliary One- and Two-Dimensional Anharmonic Vibrational Problems. In this subsection, we examine the possibility of calculating the electro-optical parameters necessary for reconstructing the absorption spectrum of the $(CH_3)_2O\cdots HF$ complex in the region of the HF stretching band. The rigorous calculation of the rovibrational parameters of this complex should include the consideration of the hindered rotation of its subunits and the addition of their angular momenta to give a total angular momentum. Such a complicated problem was beyond the scope of this study because its solution is expedient provided that an extremely accurate potential energy surface dependent on all of the intermolecular degrees of freedom is available. We used a simpler approach that was already applied for the $H_2O\cdots HF$ complex[12] and proved to be adequate for describing the bending and stretching vibrations. Along with the HF stretch, we considered the intermolecular stretch and four librations of monomers in perpendicular planes (the in-plane librations of the B_1 symmetry type and out-of-plane librations of the B_2 type). This approach allowed us to take into account the influence of all five intermolecular degrees of freedom on the HF stretching vibration. We used the following vibrational coordinates. The internal vibration of HF in the complex is described by the normal coordinate q_1 of an isolated HF molecule. The H-bond stretching vibration is described by the normal coordinate q_3 of a hypothetical diatomic molecule obtained by placing the mass of each subunit at its center of gravity. For simplicity, we assume that the librational motions of two monomers in different planes are independent. The motions of subunits in the same plane are coupled to each other through the potential energy. The kinetic energy operators for all four librations have the same form and are expressed in terms of components of the angular momentum and the moment of inertia of a subunit for the corresponding rotation axis. These librations are described by four angles θ_1, θ_2, θ_3, and θ_4. The variables θ_1 and θ_2 describe the out-of-plane librations of monomers in the plane of Figure 3, and θ_3 and θ_4 describe the in-plane librations. The coordinates thus chosen reflect the structure of the complex and allow us to obtain a sufficiently exact kinetic energy operator for the large-amplitude librational motions. The six-dimensional (6D) vibrational Hamiltonian of a complex is represented in the form

$$H = -\frac{\hbar^2}{2}\sum_k \frac{d^2}{dq_k^2} + \sum_j \frac{M_j^2}{2I_j} + V(q_1,q_3,\theta_1,\theta_2,\theta_3,\theta_4) \quad (6)$$

where $\hbar$ is Planck's constant, k numbers the two mass-weighted normal coordinates, j refers to the four angles, M_j^2 is the square of an angular momentum component, I_j is the component of the moment of inertia of a subunit, and $V(q_1,q_3,\theta_1,\theta_2,\theta_3,\theta_4)$ is the potential energy of a complex. In evaluating the quantities I_j corresponding to the four librations in question, we used the optimized geometrical parameters of monomers in the complex.

In the space of these coordinates, we obtained the variational solutions of anharmonic problems of different dimensionality starting with 1D problems. For these purposes, we computed sections of the PES and the dipole moment components. The Hamiltonians of these problems contained the corresponding components of the total kinetic energy operator. The vibrational wave functions sought were represented in the form of expansions in basis functions. For the 1D problems, the Legendre polynomials $P_l(\cos\theta_j)$ ($l = 0-29$) or the harmonic oscillator functions with $v = 0-9$ were taken to be the basis functions. In the multidimensional cases, we used the products of 1D basis functions. The energy levels and the expansion coefficients for the wave functions were obtained by solving the systems of secular equations. The matrix elements of kinetic energy operators were evaluated analytically, and the matrix elements of the potential energy were computed by Gauss−Legendre or Gauss−Hermite quadratures. The details of the computational procedures are reported in our earlier papers.[11,12]

The variational solution of the 1D anharmonic problem for the HF stretching vibration in the complex at equilibrium values of the other vibrational coordinates yields values of 3435 and 6609 cm^{-1} for the fundamental frequency and its first overtone.

The first value is in good agreement with the experimental[10] value of 3428.5 cm^{-1}. Possibly, this agreement is, to some extent, a result of mutual compensation of inaccuracies introduced in the 1D calculation by neglecting the influence of other vibrations on the ν_1 mode. The decrease in the ν_{HF} frequency upon complexation predicted by the 1D calculation equals 544 cm^{-1}, which agrees with the experimental values of 505 and 529 cm^{-1} obtained in the studies.[5,10]

The solution of the 1D problem for the $\nu_6(B_2)$ libration of $(CH_3)_2O$ at $\theta_2 = 0$ and the equilibrium values of the other variables gives a sequence of states which are even or odd under the change in the sign of θ_1. The energies of the first six states are 52.03 (the ground state even in θ_1), 52.20, 147.58, 153.47, 216.21, and 251.14 cm^{-1}. One can see that the even and odd levels lying below the barrier of 196 cm^{-1} form pairs with a small splitting, but then, the spacing between the components increases. This means that the ground vibrational state can be considered to be doubly degenerate due to the presence of an effective C_{2v} symmetry (this assumption is made in semiempirical calculations), but this is not the case for the excited states. In the same way, the following 1D anharmonic frequencies were obtained for the other intermolecular modes. The $v_3 = 0 \rightarrow 1$ transition frequency is equal to 189 cm^{-1}, which is close to the experimental estimate[5] of 185 cm^{-1}. The transitions between the ground state and the excited states of the $\nu_6(B_1)$ libration of dimethylether have frequencies of 93, 204, 326 cm^{-1}, and so forth. The frequencies of the fundamental and first overtone transitions between the librational states of HF are 764 and 1452 cm^{-1} for the in-plane libration and 635 and 1225 cm^{-1} for the out-of-plane libration.

To examine the mutual influence of the vibrational degrees of freedom of $(CH_3)_2O\cdots HF$, we considered a number of 2D vibrational problems with the nonempirical potentials dependent on two variables. The solution of the (ν_3, $\nu_6(B_2)$) problem showed that, unlike the $H_2O\cdots HF$ complex, the behavior of the $\nu_6(B_2)$ motion in $(CH_3)_2O\cdots HF$ changes qualitatively under the action of the other vibrations. For the system (ν_3, $\nu_6(B_2)$), the frequencies of transitions from the ground state to the first six excited states are 15.1, 52.2, 93.1, 139.4, 189.8, and 192.5 cm^{-1}. The first five excited states are associated with librational excitations of the ether molecule, with increasing contributions of excitation of the ν_3 mode. The transition at 192.5 cm^{-1} is identified as the $v_3 = 0 \rightarrow 1$ transition strongly perturbed by the librational motion. Note that the librational states of different symmetry do not form pairs. This is explained by the strong dependence of the potential for the $\nu_6(B_2)$ vibration on the H-bond length, in particular, by the significant increase in the barrier height as the intermolecular separation decreases. This is seen well in Figure 4 where the potential energy of $(CH_3)_2O\cdots HF$ is shown as a function of angle θ_1 and distance $\Delta R = R - R_e$, where R_e is the equilibrium separation between the centers of gravity of the monomers. This form of the 2D potential causes a significant mixing of librational and stretching modes. As compared to the case of the related complex $H_2O\cdots HF$, where this effect is weaker, the strong mixing of modes in $(CH_3)_2O\cdots HF$ is partially explained by the relatively small value of the rotational constant of $(CH_3)_2O$.

For the (ν_1, $\nu_6(B_2)$) system, the frequencies of transitions from the ground state to the first five excited states are 5.1, 62, 99, 152, and 208 cm^{-1}. These are transitions to the excited states of the $\nu_6(B_2)$ mode. We see that the interaction of the ν_1 and $\nu_6(B_2)$ modes also violates the approximate degeneracy of the neighboring librational states of different symmetry. This interaction does not virtually affect the 1D value of the ν_1 frequency.

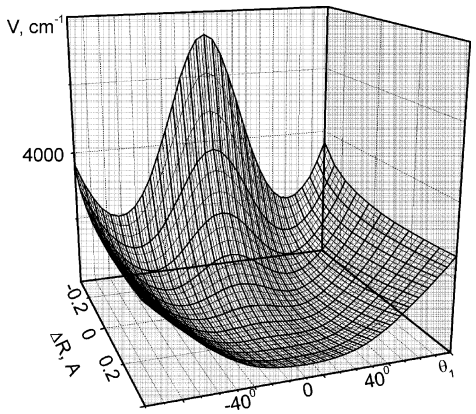

Figure 4. Potential energy of the $(CH_3)_2O\cdots HF$ complex as a function of ΔR and θ_1. Angle θ_1 describes the librational mode of $(CH_3)_2O$ in the complex, and $\Delta R = R - R_e$ is the change in the center of mass separation relative its equilibrium value.

The variational solution of the 2D ($\nu_5(B_2)$, $\nu_6(B_2)$) problem yields the energy levels symmetric or antisymmetric with respect to simultaneous changes of the signs of angles θ_1 and θ_2. These two modes are strongly coupled through the potential energy. In particular, when the symmetry axis of one partner deviates from the line joining the molecular centers of mass, the 1D potential for rotation of the other partner loses its symmetry. Despite the strong mixing of 1D motions, several low-lying excited states can be associated with the predominant excitation of the libration of one partner. The first five excited states are associated with excitations of the $\nu_6(B_2)$ mode. The frequencies of transitions to these states from the ground state are 0.42, 67, 77, 120, and 155 cm^{-1}. Note that these frequencies differ significantly from those obtained above. Due to the interaction with the $\nu_6(B_2)$ mode, the fundamental frequency of the $\nu_5(B_2)$ mode is enhanced from the 1D value of 635 cm^{-1} to a value of 659 cm^{-1}.

The results of auxiliary 1D and 2D calculations show that the $\nu_6(B_2)$ vibration, which plays an important role in the formation of the ν_1 band shape of the $(CH_3)_2O$ $(CH_3)_2O\cdots HF$ complex, is strongly perturbed by the ν_1, ν_3, and $\nu_5(B_2)$ vibrations. This suggests that, unlike the case of the $H_2O\cdots HF$ complex, it is necessary to solve at least the 4D problem (ν_1, ν_3, $\nu_5(B_2)$, $\nu_6(B_2)$) to derive the electro-optical parameters for the $(CH_3)_2O\cdots HF$ complex. To complete the picture, we note that the solution of the 2D ($\nu_5(B_1)$, $\nu_6(B_1)$) problem at the equilibrium values of other variables gives the values of 34.9, 73.7, and 118.0 cm^{-1} for the fundamental and two overtone frequencies of the $\nu_6(B_1)$ mode. These values are considerably lower than those of the 1D results. The fundamental transition frequency of the $\nu_5(B_1)$ mode (764.5 cm^{-1}) is slightly above the 1D value. A similar effect of the interaction of the in-plane librations was observed earlier[12] for the $H_2O\cdots HF$ complex.

(3) Solution of the Four-Dimensional Vibrational Problem (ν_1, ν_3, $\nu_5(B_2)$, $\nu_6(B_2)$). The solution of the 4D problem (ν_1, ν_3, $\nu_5(B_2)$, $\nu_6(B_2)$) presents significant difficulties. This is caused by the necessity to compute the potential energy and dipole moment components at a large number of points in the space of nuclear configurations. With the use of the Legendre and Hermite polynomials $P_{33}(\cos\theta_j)$ and $H_{11}(q_k)$ in the quadrature method, the total number of points is as large as 67881. The required set of values of the potential energy and dipole moment

components was obtained as follows. The dependence of the potential energy on each variable was examined for typical values of other coordinates, the regions of 4D space where the energy should be calculated accurately were determined, and the possibility of approximating the energy values in other regions was examined. The resulting 4D potential surface was constructed for $-90 \leq \theta_1,\theta_2 \leq 90°$, $0.60 \leq r(\mathrm{HF}) \leq 1.3$ Å, and the distance between the centers of mass of the monomers $2.6 \leq R \leq 3.5$ Å by using interpolation and extrapolation procedures on the basis of accurate values calculated at 5790 reference points.

One more difficulty of the variational solutions of multidimensional problems is associated with the large number of basis functions. With 10 basis functions for the stretching modes and 30 functions for librations, the number of 4D basis functions is 90 000. The basis set size was minimized without a loss in accuracy by solving a 2D problem for two librations at the equilibrium values of the intermolecular distance and r(HF). Then, several tens of 2D solutions including the ground state and the states corresponding to librational excitations of each monomer and of both monomers were chosen and multiplied by 100 products of 1D stretching basis functions. It was found that the 4D basis sets containing about 3000 symmetry-adapted functions are sufficiently complete in the sense that a further increase in the number of functions virtually does not change the energy levels and transition frequencies of interest to us.

The main part of electro-optical parameters necessary to reconstruct the absorption spectrum of the $(CH_3)_2O\cdots HF$ complex in the region of the ν_1 band was obtained from the solution of the 4D vibrational problem (ν_1, ν_3, $\nu_5(B_2)$, $\nu_6(B_2)$). In this problem, the librations of the B_1 type are ignored. A possible inclusion of the B_1-type librations should weaken the complex since they violate the most favorable mutual orientation of partners. For this reason, some effects of hydrogen bonding can be overestimated in the 4D calculation. In particular, the frequency of the intermolecular stretch and the anharmonic coupling of vibrational degrees of freedom will be overestimated, but the HF stretch frequency will be underestimated.

The zero-point energy of the system (ν_1, ν_3, $\nu_5(B_2)$, $\nu_6(B_2)$) is equal to 2303.4 cm^{-1}. The first antisymmetric 4D state lies 0.16 cm^{-1} above the ground (symmetric) state. The energies of the following four pairs of states are 47.68 (55.28), 86.08 (114.05), 145.09 (188.83), and 204.65 (205.25) cm^{-1}. The energies of the antisymmetric states are shown in parentheses. The first three pairs are the excited states of the $\nu_6(B_2)$ mode. The last pair is associated with excitations of the ν_3 mode. One can see that the tunneling splitting of the librational states increases with the increasing number of a pair. It is evident that this set of librational energy levels is difficult to describe by an expansion in powers of the quantum numbers. This fact points out the vulnerability of using simple semiempirical schemes for reconstructing the spectrum of this complex. The $v_3 = 1$ state energy (204.65 cm^{-1}) is considerably higher than the 1D value of 189.0 cm^{-1} and the 2D value of 192.5 cm^{-1} obtained in the (ν_3, $\nu_6(B_2)$) problem. This increase in the ν_3 energy is explained by the fact that in the 4D problem, the average value of r(HF) is larger and, consequently, the H bond becomes stronger. Note that the tunneling splitting of the pairs of levels with $v_3 = 1$ is equal to 0.6 cm^{-1} both for $v_1 = 0$ and for $v_1 = 1$.

Unlike the case of the weaker complex of HF with water, the assignment of states associated with the excitation of the ν_1 and low-frequency modes encounters significant difficulties. Judging from the expansion coefficients of the wave functions, only a few excited states can be unambiguously associated with excitations of 1D oscillators. Because of the significant intermode interaction in the $(CH_3)_2O\cdots HF$ complex, the 1D vibrations are so strongly perturbed that none of the expansion coefficients are predominant. In such cases, it is necessary to examine the nodal structure of sections of the wave functions, for example, in the (R, r) and (θ_1, θ_2) planes. However, for the states involving excitations of the ν_1 and ν_3 modes, the use of this method is difficult. In these cases, the wave functions have extrema in several regions of the (R, r) plane. Since the degree of mixing of 2D angular wave functions strongly depends on values of R and r, the nodal pattern of a 4D solution in the plane of two angles can change from one set of R and r to another. Let us demonstrate this situation for the example of the $|v_1v_3v_5(B_2)v_6(B_2)\rangle = |1100\rangle$ state. The 2D section of the wave function in the (R, r) plane for the equilibrium values of angles presented in Figure 5 is undoubtedly indicative of simultaneous excitation of the ν_1 and ν_3 modes. Figure 6A shows a wave function section in the (θ_1, θ_2) plane for the equilibrium values of R and r. This pattern corresponds to the doubly excited $\nu_6(B_2)$ state (the first even excited state). However, the section in the (θ_1, θ_2) plane calculated at the values of R and r averaged over this state (Figure 6B), which is more justified, does not show any excitations of the angular oscillators. The two extrema of the wave function with the same sign are associated with two wells of the potential for the $\nu_6(B_2)$ vibration. In identifying such states, it is useful to calculate the average values of R and r and the probabilities of transition to the state in question from a known initial state.

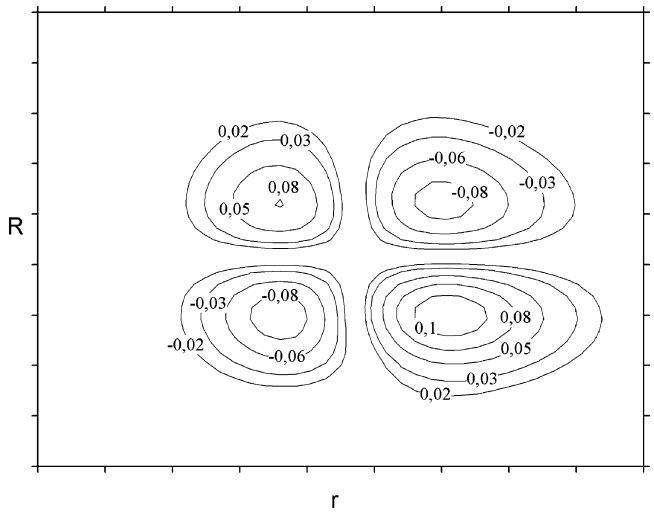

Figure 5. Two-dimensional section of the wave function of the $|v_1v_3v_5(B_2)v_6(B_2)\rangle = |1100\rangle$ state in the (R, r) plane for the equilibrium values of θ_1 and θ_2.

The integral intensities for transitions between vibrational states were calculated by the formula

$$S = 2.50643\nu[\langle i|\mu_x|f\rangle^2 + \langle i|\mu_y|f\rangle^2 + \langle i|\mu_z|f\rangle^2] \qquad (7)$$

Here, S is the absorption intensity (in km mol^{-1}) for a transition between the initial state i and a final state f and ν is the transition frequency (in cm^{-1}); $\langle i|\mu_x|f\rangle$, $\langle i|\mu_y|f\rangle$, and $\langle i|\mu_z|f\rangle$ are the dipole moment components (in D). To reduce the computer time, the last quantities were calculated in the Hartree−Fock approximation. In the analogous calculation of the spectrum of the $H_2O\cdots HF$ complex,[12] it was shown that the average values of a dipole moment and the transition dipole moments computed in the Hartree−Fock approximation are larger than the MP2 values. However, the relative intensity values of different spectral

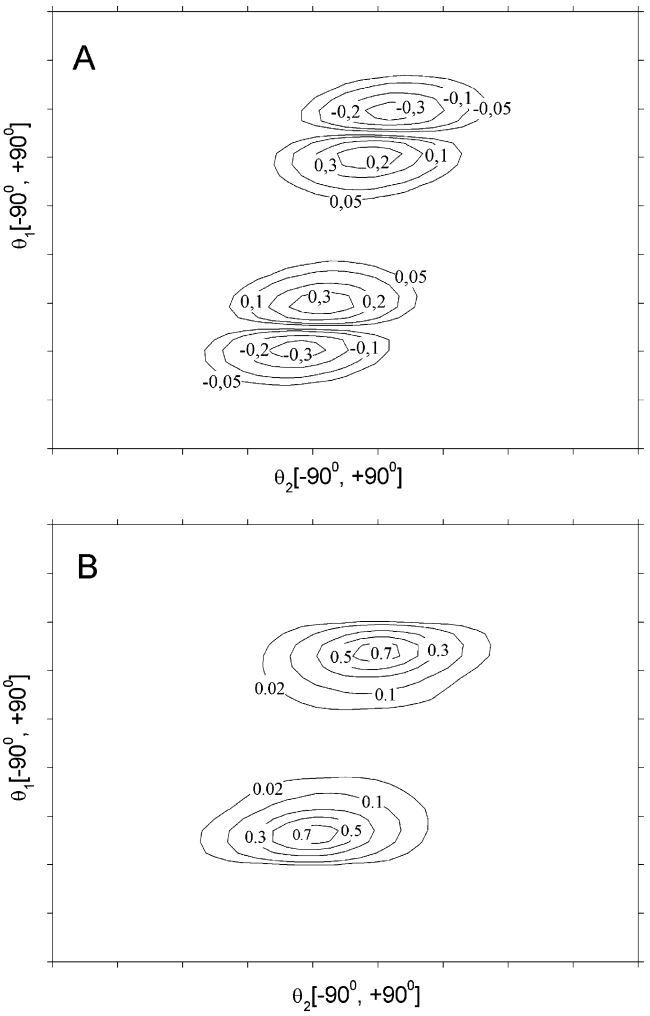

Figure 6. Two-dimensional section of the wave function of the $|v_1v_3v_5(B_2)v_6(B_2)\rangle = |1100\rangle$ state in the (θ_1, θ_2) plane for the equilibrium values of R and r (A) and for the values of R and r averaged over the $|1100\rangle$ state (B).

transitions are virtually the same in both approximations. Thus, to reconstruct the spectrum in relative units, it suffices to calculate the transition dipole moments in the Hartree−Fock approximation. This fact was confirmed here in auxiliary 2D calculations of $(CH_3)_2O\cdots HF$ by computing the dipole moment surface in two approximations.

Table 2 lists the frequencies and intensities for transitions that are the most important in explaining the ν_1 band shape. The parameters of transitions involving excitations of the $\nu_5(B_2)$ mode are omitted since these transitions are of minor importance in the formation of the spectrum studied. Therefore, in what follows, the states are denoted by the quantum numbers $|v_1\ v_3\ v_6(B_2)\rangle$. The symmetric and antisymmetric states of the $\nu_6(B_2)$ mode are labeled by the quantum number $v_6(B_2)$. This number is even for the symmetric states and odd for the antisymmetric states. The transitions listed in Table 2 occur between the states of the same symmetry under a simultaneous change of the signs of θ_1 and θ_2. The calculation showed that the electric dipole moments of transitions between the states of different angular symmetry are significant provided the degree of excitation of the stretching modes is the same in the initial and final states. Otherwise, the transition dipole moment is, on average, smaller by two orders of magnitude. For example, the dipole moments of transitions from the ground symmetric state $|000\rangle$ to the antisymmetric states $|003\rangle$ and $|103\rangle$ are equal to 0.1013 and 0.0017 D, respectively. The second value is small because the domains of large values of the angular components of the 4D wave functions are located at different values of R and r in the initial and final states. It follows from Table 2 that the theoretical value of the $v_1 = 0 \rightarrow 1$ transition frequency (3424 cm^{-1}) is in good agreement with the experimental value[10] of 3428.5 cm^{-1}. The table also shows that our calculation reproduces all of the known groups[10] of hot, sum, difference, and combination transitions of a considerable intensity. Possibly, the interaction of the ν_1 and ν_3 modes can be described by the anharmonicity constant x_{13}. Using the 1D and 4D values of the ν_3 frequency (189.00 and 204.65 cm^{-1}, respectively) and the frequencies of transitions $|000\rangle \rightarrow |100\rangle$, $|010\rangle \rightarrow |110\rangle$, $|000\rangle \rightarrow |110\rangle$, and $|010\rangle \rightarrow |100\rangle$, we obtain an estimate of 30−35 cm^{-1} for x_{13}. This value is close to a value[10] of 33 cm^{-1} and larger than $x_{13} = 20$ cm^{-1} found for the $H_2O\cdots HF$ complex.[12] Comparison of the frequencies of hot, sum, and difference transitions presented in Table 2 with the data[10] suggests that the 4D frequencies of the ν_3 and $\nu_6(B_2)$ modes and the coupling between these modes and the ν_1 mode are somewhat overestimated due to ignoring the influence of the $\nu_6(B_1)$ and $\nu_5(B_1)$ vibrations.

The intensity values for the fundamental and hot transitions between the vibrational states listed in Table 2 are close to the corresponding quantities obtained for the $H_2O\cdots HF$ complex.[11] It should be noted that the sum and difference transitions in $(CH_3)_2O\cdots HF$ are also very strong. This is a result of mixing of the librational states with different numbers of excitation quanta due to the strong intermolecular interaction. In the paper,[10] the approach of overlap integrals (a counterpart of the Franck−Condon factors in the vibronic spectra) was used to determine the relative intensities of transitions. The overlap integrals were adjustable parameters, and their variational values for some transitions appeared to be more than unity. Such large effective values can appear to compensate for some limitations of the method adopted to describe the spectrum, for example, for the consideration of only one low-frequency bending mode. In the 4D calculation, there is no need for such an approach since the angular and stretching motions are considered simultaneously. Nonetheless, we attempted to estimate these factors. We found 2D (θ_1, θ_2) sections of the 4D potential at the values of R and r averaged over the ground vibrational state (3.0269 and 0.9569 Å) and over the $|100\rangle$ state (2.9408 and 1.0043 Å). The 2D problem $(\nu_5(B_2), \nu_6(B_2))$ was solved with these potentials. The squares of the overlap integrals of the angular functions obtained with the two potentials were normalized to give 1045 for the ground state solutions and 1062 for the first antisymmetric solutions. Then, this procedure gave estimates of S in km mol^{-1} for other pairs of states. The estimates thus obtained are in satisfactory agreement with the data of Table 2. For example, the following results were obtained for transitions from the $|003\rangle$ state to the states $|101\rangle$, $|103\rangle$, $|105\rangle$, and $|107\rangle$: 122 (143), 762 (740), 206 (300), and 20 (7). The corresponding 4D values are shown in parentheses. Clearly, the agreement deteriorates upon passing to higher excited bending states. Nonetheless, this simple procedure based on solutions of 2D problems can be recommended for the estimation of the relative intensities.

Table 3 presents the vibrationally averaged values of rotational constants, distances between the centers of mass of the monomers and between the O and F atoms, as well as the HF bond length. Analysis of these data shows that the trends of changes in the average values are consistent in the sense that, for example, the excitation of the ν_3 mode causes, as expected, a decrease in B, C, and r(HF) but increases Rc.-of-m. and R(O·

TABLE 2: Values of Frequencies ν (cm^{-1}) and Intensities S (km mol^{-1}) for the $|v_1v_3v_6(B_2)\rangle \rightarrow |v_1'v_3'v_6'(B_2)\rangle$ Transitions Involved in the Formation of the ν_1 Band

initial state	final state	ν	S	initial state	final state	ν	S	initial state	final state	ν	S
|000⟩	|100⟩	3424	1045	|001⟩	|101⟩	3424	1062	|010⟩	|100⟩	3220	132
—	|102⟩	3500	159	—	|103⟩	3502	150	—	|102⟩	3296	38
—	|104⟩	3561	16	—	|105⟩	3572	9	—	|110⟩	3459	755
—	|110⟩	3664	62	—	|111⟩	3664	64	—	|112⟩	3531	159
—	|112⟩	3735	3	—	|113⟩	3736	2	—	|114⟩	3578	12
|002⟩	|100⟩	3377	136	|003⟩	|101⟩	3369	143	|011⟩	|101⟩	3219	137
—	|102⟩	3452	505	—	|103⟩	3447	740	—	|103⟩	3297	39
—	|104⟩	3513	498	—	|105⟩	3517	300	—	|111⟩	3459	799
—	|106⟩	3561	52	—	|107⟩	3596	7	—	|113⟩	3531	106
—	|110⟩	3616	4	—	|111⟩	3609	5	—	|115⟩	3608	2
—	|112⟩	3687	45	—	|113⟩	3681	47	|012⟩	|102⟩	3255	30
—	|114⟩	3735	8	—	|115⟩	3758	3	—	|104⟩	3316	84
|004⟩	|100⟩	3339	35	|005⟩	|101⟩	3310	13	—	|106⟩	3363	17
—	|102⟩	3414	397	—	|103⟩	3388	269	—	|110⟩	3419	121
—	|104⟩	3474	253	—	|105⟩	3458	605	—	|112⟩	3490	389
—	|106⟩	3522	479	—	|107⟩	3538	287	—	|114⟩	3538	247
—	|112⟩	3649	16	—	|113⟩	3622	3	|013⟩	|103⟩	3245	69
—	|114⟩	3697	23	—	|115⟩	3699	45	—	|105⟩	3315	52
|006⟩	|102⟩	3355	117	|007⟩	|103⟩	3313	38	—	|107⟩	3394	23
—	|104⟩	3415	342	—	|105⟩	3383	223	—	|111⟩	3407	109
—	|106⟩	3463	436	—	|107⟩	3463	702	—	|113⟩	3479	537
—	|108⟩	3541	287	—	|109⟩	3571	178	—	|115⟩	3556	165

TABLE 3: Vibrationally Averaged Values of Rotational Constants *A*, *B*, and *C* and the Distances *R*c.-of-m., *R*(O···F), and *r*(HF) in the $|v_1\ v_3\ v_6(B_2)\rangle$ States

state	*A* (cm^{-1})	*B* (cm^{-1})	*C* (cm^{-1})	*R*c.-of-m. (Å)	*R*(O···F) (Å)	*r*(HF) (Å)
|000⟩	0.3192	0.1192	0.0918	3.0269	2.6420	0.9569
|001⟩	0.3191	0.1193	0.0919	3.0254	2.6419	0.9569
|002⟩	0.3245	0.1158	0.0894	3.0774	2.6478	0.9555
|003⟩	0.3215	0.1179	0.0909	3.0481	2.6455	0.9562
|004⟩	0.3234	0.1168	0.0901	3.0652	2.6476	0.9556
|005⟩	0.3213	0.1182	0.0911	3.0453	2.6466	0.9560
|010⟩	0.3206	0.1160	0.0898	3.0773	2.6793	0.9555
|011⟩	0.3202	0.1163	0.0899	3.0735	2.6790	0.9556
|012⟩	0.3257	0.1130	0.0876	3.1240	2.6840	0.9543
|013⟩	0.3218	0.1155	0.0894	3.0864	2.6812	0.9551
|100⟩	0.3163	0.1254	0.0958	2.9408	2.5874	1.0043
|101⟩	0.3164	0.1254	0.0957	2.9419	2.5877	1.0043
|102⟩	0.3181	0.1242	0.0949	2.9606	2.5933	1.0024
|103⟩	0.3187	0.1237	0.0946	2.9662	2.5926	1.0025
|104⟩	0.3233	0.1202	0.0921	3.0155	2.6017	1.0001
|105⟩	0.3218	0.1211	0.0928	3.0029	2.6013	1.0001
|110⟩	0.3171	0.1226	0.0940	2.9823	2.6208	1.0010
|111⟩	0.3174	0.1221	0.0937	2.9885	2.6237	1.0020
|112⟩	0.3204	0.1201	0.0922	3.0203	2.6311	0.9998
|113⟩	0.3197	0.1208	0.0927	3.0090	2.6263	0.9993

··F). The values of all quantities calculated for states with $v_6(B_2) = 1$ and 2 virtually coincide. However, the values of *A*, *B*, *C*, and *R*c.-of-m. for other pairs of symmetric and antisymmetric states can differ significantly. Upon excitation of the ν_3 and $\nu_6(B_2)$ modes, the rotational constants *B* and *C* decrease by 0.002−0.006 cm^{-1}, and the constant *A* increases by the same magnitude. On the contrary, the excitation of the ν_1 mode increases *B* and *C* and decreases *A*. These changes can be partially compensated for upon excitation of the ν_3 and $\nu_6(B_2)$ modes.

Due to the anharmonicity, the average values of *R*c.-of-m. and *r*(HF) in the ground state are larger than the equilibrium values presented in subsection (1) by 0.024 and 0.018 Å, respectively. The excitation of the $\nu_6(B_2)$ mode weakens the hydrogen bond since the mutual orientation of partners is no longer optimal. This leads to elongation of *R*c.-of-m., but this effect is not linear in $v_6(B_2)$ since the average value of θ_1 depends on the degree of excitation of $\nu_6(B_2)$ in a complicated way. These conclusions were confirmed by calculations of average values of $P_2(\cos(\theta_1))$. Excitation of the ν_3 mode increases *R*c.-of-m., and excitation of the ν_1 mode decreases this quantity. The increments are 0.0504 and −0.0861 Å, respectively. Note that in the analogous calculation of H_2O···HF,[12] it was found that the excitation of the ν_1 mode decreases the distance between the centers of mass by 0.046 Å. Interestingly, the interatomic separation *R*(O···F) is virtually independent of excitation of the $\nu_6(B_2)$ mode because the changes in *R*(O···F) resulting from changes in *R*c.-of-m. and the rotation of the ether molecule are close in magnitude but opposite in sign. This implies that to characterize an effective separation between the monomers in dimers of the type R_1B···H−AR_2, it is reasonable to use the distance between the centers of gravity rather than the distance *R*(B···A). The behavior of an average value of *R*(O···F) upon excitation of the ν_1 and ν_3 modes resembles the behavior of ⟨*R*c.-of-m.⟩. In particular, ⟨*R*(O···F)⟩ is decreased by 0.0546 Å upon the $v_1 = 0 \rightarrow 1$ transition, which is larger than a similar result of 0.041 Å obtained for H_2O···HF.[12] Our calculation shows that the decrement ΔR(O···F) = 0.22 Å adopted in the semiempirical calculation[10] is overestimated. The behavior of ⟨*r*(HF)⟩ is opposite to that of ⟨*R*c.-of-m.⟩. Upon the $v_1 = 0 \rightarrow 1$ transition, ⟨*r*(HF)⟩ increases by 0.0474 Å, which is larger than the corresponding increment of 0.0399 Å in H_2O···HF.[12]

(4) Reconstruction of the Absorption Spectrum of the $(CH_3)_2O$···HF Complex in the Region of the ν_1 Mode. The absorption spectrum of the $(CH_3)_2O$···HF complex was reconstructed as a superposition of separate rovibrational bands. Along with the contribution of the fundamental $v_1 = 0 \rightarrow 1$ transition from the ground state, the contributions of hot, sum, and difference transitions with changes in the quantum numbers of the ν_3, $\nu_6(B_1)$, and $\nu_6(B_2)$ modes were also considered. The transitions between the states of the $\nu_5(B_1)$ and $\nu_5(B_2)$ modes were ignored because their contributions are relatively small. The total number of vibrational transitions was larger than 2000. In a rigorous treatment of the rovibrational spectrum of $(CH_3)_2O$···HF, it is necessary to take into account that this complex is an asymmetric top. The asymmetric top model was successfully used in the simulation of spectra of the $(CH_2)_2S$···HF and $(CH_2)_2S$···DF heterodimers recorded in the high-precision supersonic jet expansion and cooled gas cell experiments.[22,23] The use of this model is advisable since these spectra reveal traces of the

rotational structure. The absorption spectra of the $(CH_3)_2O\cdots HF$ complex are less structured and can be described in a simpler way. In the present paper, individual rovibrational bands were calculated in the approximations of a symmetric top or a linear rotator with a rotational constants B equal to the half-sum of the real constants B and C presented in Table 3. The choice of the form and parameters of separate spectral lines is also a difficult task which requires the consideration of many mechanisms of the line broadening and line shift, including the vibrational relaxation effects because of the presence of a large number of closely spaced vibrational levels. This may be the subject of a separate study. In this calculation, we represented the rovibrational lines in the form of a Lorentzian with the half-width at half-maximum $b_0 = 1\ cm^{-1}$. In fact, this choice of b_0 is a method to smooth the fine structure, which, as a rule, is not seen in the experimental spectra. In this case, the spectra calculated in the approximations of a symmetric top and a linear rotator virtually coincide.

The main part of the vibrational energy levels, the transition frequencies and intensities, and the rotational constants of combining states were derived from the above 4D calculation. When reconstructing the spectrum, it is also necessary to take into account the $\nu_6(B_1)$ in-plane vibration. Otherwise, the number of low-frequency states is too small. Test calculations showed that the energy barrier is absent for the $\nu_5(B_1)$ and $\nu_6(B_1)$ vibrations, at least, at not too short separations between the monomers. Therefore, the description of these vibrations can be simpler than that for the ($\nu_5(B_2)$, $\nu_6(B_2)$) pair. We did not solve the 4D problem (ν_1, ν_3, $\nu_5(B_1)$, $\nu_6(B_1)$) but obtained variational solutions of the 2D problem ($\nu_5(B_1)$, $\nu_6(B_1)$) at different values of *R*c.-of-m. and *r*(HF), in particular, at the average values of these distances in the ground state and the $v_1 = 1$ excited state of the system (ν_1, ν_3, $\nu_5(B_2)$, $\nu_6(B_2)$). Similar calculations were carried out for $H_2O\cdots HF$. Comparison of the results thus obtained with the solutions of a more rigorous problem for $H_2O\cdots HF$[12] showed that it is possible to satisfactorily estimate the energies of excited states of the $\nu_6(B_1)$ mode by taking several low-lying states of the system ($\nu_5(B_1)$, $\nu_6(B_1)$) at *R*c.-of-m. and *r*(HF) averaged over the ground state of the more rigorous problem. The anharmonicity constant $x_{16(B_1)}$ can be obtained from the difference between these energy states and the analogous 2D energies found at *R*c.-of-m. and *r*(HF) averaged over the $v_1 = 1$ excited state. For the $(CH_3)_2O\cdots HF$ complex, this consideration yielded a set of slightly divergent energy levels of the $\nu_6(B_1)$ mode with the fundamental frequency of 26.7 cm^{-1} and the upper estimate of $x_{16(B_1)} = 7.5\ cm^{-1}$. The intensities of hot transitions from the $\nu_6(B_1)$ levels were obtained by using the above procedure based on the overlap integrals of 2D angular wave functions. It appeared that here, unlike the case of the $\nu_6(B_2)$ states, the diagonal overlap integrals are close to unity and the squares of nondiagonal integrals are negligible. In considering the transitions involving both the changes in the states of the 4D system (ν_1, ν_3, $\nu_5(B_2)$, $\nu_6(B_2)$) and the hot transitions from the $\nu_6(B_1)$ states, the energy levels and transition frequencies were evaluated by the additive scheme and the intensities by the recipe proposed earlier.[12] The final set of transitions used to reconstruct the spectrum may be incomplete since it does not contain transitions between symmetric and antisymmetric states of the $\nu_6(B_1)$ mode. To derive the intensities for such transitions, it is necessary to solve the 4D problem (ν_1, ν_3, $\nu_5(B_1)$, $\nu_6(B_1)$).

With the set of electro-optical parameters thus obtained, the absorption spectrum of the $(CH_3)_2O\cdots HF$ complex in the region of the ν_1 band was calculated for different temperatures. The theoretical spectra reconstructed for $T = 190$, 230, 285, and 320 K are shown in Figures 1 and 2. The theoretical spectra were normalized so that their integral optical densities coincide with the experimental values. The theoretical spectra were shifted above to avoid an overlap with the experimental curves, but they were not shifted along the frequency axis.

Discussion

The experimental spectra presented in Figures 1 and 2 show the gradual disappearance of separate spectral details and the broadening of the band shape with increasing temperature. These changes are reflected by the temperature behavior of the first and second spectral moments. The theoretical spectra reproduce both the overall shape of the experimental spectra and their position on the frequency axis. The calculation predicts the main spectral features. The peak with the lowest frequency in the central part of the spectra is associated with the *P* branch head of the fundamental transition. Its relative intensity decreases with temperature. The peaks associated with the $|00v_6(B_1)\rangle \rightarrow |10v_6(B_1)\rangle$, $|00v_6(B_2)\rangle \rightarrow |10v_6(B_2)\rangle$ hot transitions, and similar transitions from the states with $v_6(B_1) \neq 0$ and $v_6(B_2) \neq 0$ are located at higher frequencies. In our opinion, the theoretical values of the $|00v_6(B_2)\rangle \rightarrow |10v_6(B_2)\rangle$ transition frequencies are overestimated. For example, our frequency value for the $|00v_6(B_2)\rangle \rightarrow |10v_6(B_2)\rangle$ transition from the $v_6(B_2) = 2$ level (see Table 2) is higher by 12.5 cm^{-1} than the value derived by simulating the experimental spectra.[10] This fact gives rise to a high-frequency shift of hot transitions from the $\nu_6(B_2)$ excited states relative to the fundamental transition and to an appreciable shift of the central maximum of the spectrum and its broadening, especially at higher temperatures. This computational effect stems from the overestimation of the intermode coupling in the 4D calculation without taking into account the in-plane vibrations that weaken the hydrogen bond.

To verify this supposition, we solved the 3D problem (ν_1, $\nu_5(B_2)$, $\nu_6(B_2)$) at values of *R*c.-of-m. larger than its average value (3.0269 Å) in the ground state. The calculations showed that the difference between the frequencies of the transitions $|002\rangle \rightarrow |102)\rangle$ and $|000\rangle \rightarrow |100)\rangle$ (the anharmonic coupling constant for the ν_1 and $\nu_6(B_2)$ modes), whose 4D value equals 27.8 cm^{-1}, decreases with increasing *R*c.-of-m. We found from test calculations that *R*c.-of-m. should increase by about 0.07 Å, with the zero-point vibration of the $\nu_5(B_1)$ and $\nu_6(B_1)$ modes taken into account. Upon such elongation of the H bond, the difference of frequencies of the $|002\rangle \rightarrow |102)\rangle$ and $|000\rangle \rightarrow |100)\rangle$ transitions drops to 15 cm^{-1}, which is close to a value of $x_{s\delta}$ found in the simulation.[10] Then, we calculated the spectra with a set of parameters where the frequencies of the first three hot transitions from the $\nu_6(B_2)$ levels were estimated by using the anharmonicity constant equal to 15 cm^{-1}, with the intensities and all the other parameters being unchanged. It appeared that the spectra thus reconstructed are in much better agreement with the experimental data.

According to our calculation, the high-frequency maximum I is formed by the $|00v_\delta\rangle \rightarrow |11v'_\delta\rangle$ transitions with $v_\delta = v_6(B_1)$ and $v_6(B_2)$. Here, $v'_6(B_1) = v_6(B_1)$, and $v'_6(B_2) = v_6(B_2)$ and $v_6(B_2) \pm 2$. Recall that in our notation, the symmetric and antisymmetric states have different quantum numbers. Therefore, the quantum numbers of neighboring states of the same symmetry differ by two. The $|01v_\delta\rangle \rightarrow |12v'_\delta\rangle$ transitions also contribute to the absorption in this region. These contributions become larger with temperature. It is worth noting that the intensity S (eq 7) for the $|010\rangle \rightarrow |120\rangle$ transition at a frequency of 3686 cm^{-1} equals 101 km mol^{-1}, which is almost twice as

high as the intensity for the $|000\rangle \rightarrow |110\rangle$ transition. The contributions to the spectrum in region II are primarily made by the $|00v_6(B_2)\rangle \rightarrow |10v_6(B_2) + 2\rangle$ and $|01v_6(B_2)\rangle \rightarrow |11v_6(B_2) + 2\rangle$ transitions, as well as by combinations of these transitions with hot transitions from the $\nu_6(B_1)$ levels. For the reason discussed above, the calculated values of the corresponding frequencies are somewhat overestimated. Region III is formed by the $|00v_6(B_2)\rangle \rightarrow |10v_6(B_2) - 2\rangle$ and $|01v_6(B_2)\rangle \rightarrow |11v_6(B_2) - 2\rangle$ transitions. Finally, absorption region IV at frequencies below 3300 cm^{-1} is formed by the $|01v_6(B_2)\rangle \rightarrow |10\ v'_6(B_2)\rangle$ transitions with $v'_6(B_2) = v_6(B_2)$ and $v_6(B_2) + 2$. Thus, our interpretation of the experimental spectra coincides, on the whole, with the conclusions of previous studies[7,8,10] and supplements them by emphasizing the role of the $|01v_\delta\rangle \rightarrow |12\ v'_\delta\rangle$ transitions at higher temperatures.

The temperature behavior of the first and second spectral moments evaluated from the theoretical spectra is in agreement with the experimental findings. However, there are some discrepancies. The theoretical values of M_1^*, M_2^*, and $\Delta\nu_{1/2}$ are larger than the experimental data at $T = 190$ and 230 K. The reason lies in the shift and broadening of the central maximum and the increased spacing between regions I and IV of the spectrum caused by overestimating the intermode coupling in the 4D calculation. At higher temperatures, the theoretical values of M_1^*, M_2^*, and $\Delta\nu_{1/2}$ are smaller than the experimental counterparts. Possibly, this fact is explained by an insufficient number of transitions from excited states taken into account in reconstructing the spectrum. Only transitions from the states of the 4D system (ν_1, ν_3, $\nu_5(B_2)$, $\nu_6(B_2)$) lying below 450 cm^{-1} were identified and considered. Transitions from the higher lying states may contribute to the shoulders and wings of the central part of spectrum and to the subbands I and IV.

Conclusions

The absorption spectra of the $(CH_3)_2O\cdots HF$ complex in the ν_1 region were recorded in the gas phase within a wide temperature interval of $T = 190-340$ K at a resolution of 0.1 cm^{-1}. They are used to analyze both separate features of the band shape and integral spectral characteristics. The temperature dependences of the first and second normalized spectral moments are reliably determined. The spectra studied are reconstructed nonempirically by solving a number of 1D−4D vibrational Schrödinger equations in the space of two stretching and four bending coordinates. These equations are solved by the variational method with the potential energy surfaces calculated at the MP2 6-311++G(2d,2p) level, with the basis set superposition error taken into account. The sufficiently complete set of the vibrational energy levels, transition frequencies and absolute intensities, and the rotational constants was derived. The theoretical spectra reconstructed with these electro-optical parameters are in good agreement with the experimental data. They reproduce both the overall shape and separate components of the spectra. The fundamental frequency value of 3424 cm^{-1} obtained in the calculation is close to the experimental value[10] of 3428.5 cm^{-1}.

The calculation shows that the intermolecular interaction in the $(CH_3)_2O\cdots HF$ complex is considerably stronger than that in the related $H_2O\cdots HF$ complex. This conclusion is confirmed by the behavior of the potential energy surfaces, the larger ν_1 frequency shift upon complexation, and the higher intensities of the sum and difference transitions as compared to the corresponding characteristics of $H_2O\cdots HF$. In the $(CH_3)_2O\cdots HF$ complex, unlike the case of the $H_2O\cdots HF$ complex, the frequencies of hot transitions from excited $\nu_6(B_2)$ levels are higher than the fundamental ν_1 frequency. This distinction is explained by the stronger intermode coupling in $(CH_3)_2O\cdots HF$ and the smaller rotational constant of $(CH_3)_2O$. Among the results obtained, of interest are the vibrationally averaged values of geometrical parameters and rotational constants evaluated for many states using the 4D wave functions. To conclude, we note that it is desirable to carry out a more complete 6D calculation of this complex involving the HF stretch and five intermolecular degrees of freedom to obtain more accurate electro-optical parameters.

Acknowledgment. This study was supported by the Russian Foundation for Basic Research, Grant No. 06-03-32073. The authors are grateful to the Telecommunication Center of St. Petersburg State University for providing computer time.

References and Notes

(1) Arnold, J.; Millen, D. J. *J. Chem. Soc.* **1965**, 503.

(2) Bevan, J. W.; Martineau, B.; Sandorfy, C. *Can. J. Chem.* **1979**, *57*, 1341.

(3) Millen, D. J.; Schrems, O. *Chem. Phys. Lett.* **1983**, *101*, 320.

(4) Cousi, M.; Calve, J.; Huong, P. V.; Lascome, J. *J. Mol. Struct.* **1970**, *5*, 363.

(5) Thomas, R. K. *Proc. R. Soc. London, Ser. A* **1971**, *322*, 137.

(6) Andrews, L.; Johnson, G. L.; Davis, S. R. *J. Phys. Chem.* **1985**, *89*, 1710.

(7) Tokhadze, K. G.; Bernikov, M. A.; Voronin, A. Yu.; Tylets, N. N. *Opt. Spectrosc.* **1988**, *65*, 322.

(8) Tokhadze, K. G.; Bernikov, M. A.; Voronin, Yu, A. *Opt. Spectrosc.* **1992**, *73*, 167.

(9) Shchepkin, D. N. *J. Mol. Struct.* **1987**, *156*, 304.

(10) Asselin, P.; Soulard, P.; Alikhani, M. E.; Perchard, J. P. *Chem. Phys.* **2000**, *256*, 195.

(11) Bulychev, V. P.; Gromova, E. I.; Tokhadze, K. G. *Opt. Spectrosc.* **2004**, *96*, 774.

(12) Bulychev, V. P.; Grigoriev, I. M.; Gromova, E. I.; Tokhadze, K. G. *Phys. Chem. Chem. P*hys. **2005**, *7*, 2266.

(13) Goubet, M.; Madebene, B.; Lewerenz, M. *Chimia* **2004**, *58*, 291.

(14) Smith, D. F. *J. Chem. Phys.* **1958**, *28*, 1040.

(15) Bulychev, V. P.; Mielke, Z.; Tokhadze, K. G.; Utkina, S. S. *Opt. Spectrosc.* **1999**, *86*, 352.

(16) Gordon, R. G. *J. Chem. Phys.* **1964**, *41*, 1819.

(17) Molecular Cryospectroscopy. In *Advances in Spectroscopy*; Clark, R. J. H., Hester, R. E., Eds.; Wiley: New York, 1995; 23.

(18) Frisch, M. J.; Trucks, G. W.; Schlegel, H. B.; Scuseria, G. E.; Robb, M. A.; Cheeseman, J. R.; Montgomery, J. A., Jr.; Vreven, T.; Kudin, K. N.; Burant, J. C.; Millam, J. M.; Iyengar, S. S.; Tomasi, J.; Barone, V.; Mennucci, B.; Cossi, M.; Scalmani, G.; Rega, N.; Petersson, G. A.; Nakatsuji, H.; Hada, M.; Ehara, M.; Toyota, K.; Fukuda, R.; Hasegawa, J.; Ishida, M.; Nakajima, T.; Honda, Y.; Kitao, O.; Nakai, H.; Klene, M.; Li, X.; Knox, J. E.; Hratchian, H. P.; Cross, J. B.; Bakken, V.; Adamo, C.; Jaramillo, J.; Gomperts, R.; Stratmann, R. E.; Yazyev, O.; Austin, A. J.; Cammi, R.; Pomelli, C.; Ochterski, J. W.; Ayala, P. Y.; Morokuma, K.; Voth, G. A.; Salvador, P.; Dannenberg, J. J.; Zakrzewski, V. G.; Dapprich, S.; Daniels, A. D.; Strain, M. C.; Farkas, O.; Malick, D. K.; Rabuck, A. D.; Raghavachari, K.; Foresman, J. B.; Ortiz, J. V.; Cui, Q.; Baboul, A. G.; Clifford, S.; Cioslowski, J.; Stefanov, B. B.; Liu, G.; Liashenko, A.; Piskorz, P.; Komaromi, I.; Martin, R. L.; Fox, D. J.; Keith, T.; Al-Laham, M. A.; Peng, C. Y.; Nanayakkara, A.; Challacombe, M.; Gill, P. M. W.; Johnson, B.; Chen, W.; Wong, M. W.; Gonzalez, C.; Pople, J. A. *Gaussian 03*, revision B.04; Gaussian, Inc.: Pittsburgh, PA, 2004.

(19) Boys, S. F.; Bernardi, F. *Mol. Phys.* **1970**, *19*, 553.

(20) Asselin, P.; Goubet, M.; Latajka, Z.; Soulard, P.; Lewerenz, M. *Phys. Chem. Chem. Phys.* **2005**, *7*, 592.

(21) Salai Cheettu Ammal, S.; Venuvanalingam, P. *J. Chem. Soc., Faraday Trans.* **1998**, *94*, 2669.

(22) Asselin, P.; Goubet, M.; Lewerenz, M.; Soulard, P.; Perchard, J. P. *J. Chem. Phys.* **2004**, *121*, 5241.

(23) Goubet, M.; Asselin, P.; Soulard, P.; Lewerenz, M.; Latajka, Z. *J. Chem. Phys.* **2004**, *121*, 7784.